THE JOURNAL OF PHYSICAL CHEMISTRY B

Article

pubs.acs.org/JPCB

Temperature Dependence of Triplet–Triplet Annihilation Upconversion in Phospholipid Membranes

Sven H. C. Askes,[†] Philip Brodie,[†] Gilles Bruylants,[‡] and Sylvestre Bonnet*[,†]

[†]Leiden Institute of Chemistry, Gorlaeus Laboratories, Leiden University, P.O. Box 9502, 2300 RA Leiden, The Netherlands

[‡]Engineering of Molecular NanoSystems, Université Libre de Bruxelles, 50 av. F.D. Roosevelt, 1050 Brussels, Belgium

Supporting Information

ABSTRACT: Understanding the temperature dependency of triplet–triplet annihilation upconversion (TTA-UC) is important for optimizing biological applications of upconversion. Here the temperature dependency of red-to-blue TTA-UC is reported in a variety of neutral PEGylated phospholipid liposomes. In these systems a delicate balance between lateral diffusion rate of the dyes, annihilator aggregation, and sensitizer self-quenching leads to a volcano plot, with the maximum upconversion intensity occurring near the main order–disorder transition temperature of the lipid membrane.

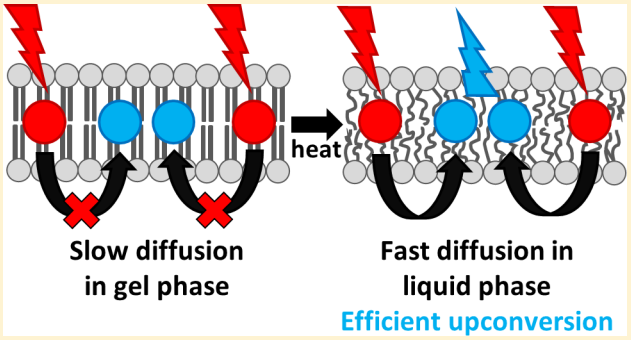

INTRODUCTION

Light upconversion is the generation of high-energy photons from low-energy photons, for example, the conversion of red light to blue light. Generating upconverted light can be achieved using different systems such as two-photon absorption dyes, rare earth-doped materials or nanoparticles, and triplet–triplet annihilation (TTA-UC). Among these systems, TTA-UC offers many advantages: it works at low excitation power (down to 1 mW cm^{-2}), it uses sensitizers having high molar absorptivity, and the obtained upconversion quantum yields are high, typically 1–5% in aqueous solution.[1] Since its popularization more than a decade ago,[2] TTA-UC has been used in many applications such as photocatalysis,[3] solar energy harvesting,[4] drug delivery and activation,[5] and luminescence bioimaging.[1a,6] TTA-UC is based on the photophysical interplay of photosensitizer and annihilator chromophores (see Figure S1).[7] The photosensitizer absorbs low energy light, after which intersystem crossing leads to a long-lived triplet state. The energy of this triplet state is transferred to the annihilator upon diffusional collision by means of triplet–triplet energy transfer (TTET); a succession of TTET leads to a concentration buildup of long-lived triplet-state annihilators. Two triplet-state annihilators can then perform triplet–triplet annihilation upconversion, in which one of them departs with the energy of both triplet states, to reach a high-energy singlet state. Finally, this singlet excited state returns to the ground state by emission of a high-energy photon, thus realizing light upconversion.

TTA-UC has been demonstrated in an extensive assortment of organic, inorganic, and/or supramolecular materials,[1c,8] as well as in nano- or microsized particles.[9] Among the various applications of TTA-UC, some of them require to operate above room temperature, such as bioimaging and phototherapy. It is thus important to understand the temperature dependency of upconversion efficiency. Because TTET and TTA occur via molecular collisions, these processes are highly dependent on molecular diffusion; the efficiency of TTA-UC was reported as being greatly influenced by the fluidity of the matrix containing the dyes, and hence by the temperature.[10] For many materials, a higher temperature leads to a higher fluidity, and therefore to higher TTA-UC efficiency. For example, green-to-blue TTA-UC in a rubbery polymer matrix was only visible above the glass transition temperature of the material, where the matrix becomes more fluid.[11] However, diffusion is not the only important factor. First of all, temperature-dependent chemical phenomena such as dye aggregation may affect upconversion as well: counter-intuitively, it was recently shown that at lower temperatures, mixed aggregation of sensitizer and annihilator molecules in diluted conditions resulted in higher TTA-UC efficiency.[12] It has also been shown that upconversion in gel matrices decreased at higher temperatures due to temperature-dependent disassembly of the host material.[8c] Overall, understanding the temperature dependence of all chemical and physical properties of a given matrix is necessary for optimizing upconversion.

Our group recently demonstrated that green-to-blue and red-to-blue TTA-UC can be realized in the phospholipid membrane of neutral PEGylated liposomes composed of 1,2-dimyristoyl-*sn*-glycero-3-phosphocholine (DMPC). This knowledge was later used for the activation of photoactivatable chemotherapeutic agents in the photodynamic window.[5] In our initial studies it was reported that the upconversion intensity was reversibly affected by changes in temperature.[5b] Upon heating the sample from 15 to 25 °C the upconversion intensity increased significantly,

Received: October 4, 2016
Revised: December 11, 2016
Published: January 6, 2017

DOI: 10.1021/acs.jpcb.6b10039
J. Phys. Chem. B 2017, 121, 780–786

which we interpreted as a consequence of the gel-to-liquid crystalline phase transition temperature (T_m) of the DMPC lipid bilayer. Upon raising the temperature above T_m the molecular diffusion of the dyes in the membrane is expected to increase greatly, which should lead to higher TTET and TTA rates, and thus higher TTA-UC efficiencies. In this work, we systematically investigated the temperature dependency of TTA-UC in neutral PEGylated liposomes made of different lipids with different transition temperatures T_m, to optimize the lipid composition of red-to-blue TTA-UC drug-delivery systems functioning at human body temperature.

EXPERIMENTAL SECTION

General. Palladium tetraphenyltetrabenzoporphyrin (**1**) was purchased from Bio-Connect (Huissen, The Netherlands). Perylene (**2**) was purchased from Sigma-Aldrich Chemie BV (Zwijndrecht, The Netherlands). All lipids were purchased from either Lipoid GmbH (Ludwigshafen, Germany) or Avanti Polar Lipids (Alabaster, AL, USA) and stored at −18 °C. Dulbecco's phosphate buffered saline (DPBS) was purchased from Sigma-Aldrich and had a formulation of 8 g·L^{-1} NaCl, 0.2 g·L^{-1} KCl, 0.2 g·L^{-1} KH_2PO_4, and 1.15 g·L^{-1} K_2HPO_4 with a pH of 7.1−7.5.

Liposome Assembly. All liposome formulations were prepared by the classical hydration-extrusion method. As an example, the preparation of liposome sample **O12** is described here. Aliquots of chloroform stock solutions containing the liposome constituents were added together in a flask to obtain a solution with 5.0 μmol DOPC, 0.20 μmol DSPE-mPEG-2000, 2.5 nmol compound **1**, and 25 nmol compound **2**. The organic solvent was removed by rotary evaporation and subsequently under high vacuum for at least 30 min to create a lipid film. 1.0 mL DPBS buffer, with or without 0.3 M sodium sulfite, was added and the lipid film was hydrated by 4 cycles of freezing the flask in liquid nitrogen and thawing in warm water (60 °C). The resulting dispersion was extruded through a Whatman Nuclepore 0.2 μm polycarbonate filter at least 10 °C above the main phase transition temperature of the lipid for at least 11 times using a mini-extruder from Avanti Polar Lipids, Inc. (Alabaster, Alabama, USA), fitted with two 1001RN gastight syringes from Hamilton (Bonaduz, Switzerland). Warning: heating the gastight syringes to 50−70 °C will cause the Teflon plunger to leak at room temperature—it is advised to use one set of syringes for hot extrusion only! The number of extrusions was always odd to prevent any unextruded material ending up in the final liposome sample. The extrusion filter remained practically colorless after extrusion, suggesting near-complete inclusion of the dyes in the lipid bilayer. Liposomes were stored in the dark at 4 °C and used within 7 days. The average liposome size and polydispersity index were measured with a Malvern Instruments Zetasizer Nano-S machine, operating with a wavelength of 632 nm.

Differential Scanning Calorimetry. Differential scanning calorimetry (DSC) was performed on a TA Instruments (DE, USA) nano-DSC III instrument in the range of 5 to 50 °C with a scanning rate of 1 °C min^{-1} at 3 atm. The capillary cell (V = 300 μL) was filled with the liposome solution (lipid bulk concentration of 5 mM), and the reference cell was filled with PBS buffer solution. A blank measurement was performed with PBS buffer. The liposome dispersions were degassed for 10−15 min prior to measurement on a Nalgene degassing station. For each sample, at least two cycles of heating and cooling were performed with 10 min of thermal equilibration between the ramps. The machine was cleaned beforehand with 50% formic acid and rinsed thoroughly with Milli-Q water. The thermograms were processed and analyzed using NanoAnalyze software from TA Instruments.

Absorption and Emission Spectroscopy. Absorption and emission spectroscopy was conducted in a custom-built setup (Figure S2). All optical parts were connected with FC-UV*xxx*-2 (*xxx* = 200, 400, 600) optical fibers from Avantes (Apeldoorn, The Netherlands), with a diameter of 200−600 μm, respectively, and that were suitable for the UV−vis range (200−800 nm). Typically, 2.25 mL of sample was placed in a 111-OS macro fluorescence cuvette from Hellma in a CUV-UV/vis-TC temperature-controlled cuvette holder with stirring from Avantes. Deoxygenated toluene samples were prepared in a glovebox in a sealed fluorescence cuvette. The cuvette holder temperature was controlled with a TC-125 controller and T-app computer software from Quantum Northwest (Liberty Lake, WA, USA), while the sample temperature was measured with an Omega RDXL4SD thermometer with a K-type probe submerged in the sample. The sample was excited with a 10 mW collimated 630 nm laser light beam (4 mm beam diameter, 80 mW cm^{-2}) from a Diomed 630 nm PDT laser. The 630 nm light was filtered through a 630 nm band-pass filter (FB630−10 from Thorlabs, Dachau/Munich, Germany) put between the laser and the sample. The excitation power was controlled using the laser control in combination with a NDL-25C-4 variable neutral density filter (Thorlabs), and measured using a S310C thermal sensor connected to a PM100USB power meter (Thorlabs). UV−vis absorption spectra were measured using an Avalight-DHc halogen-deuterium lamp (Avantes) as light source and a 2048L StarLine spectrometer (Avantes) as detector, both connected to the cuvette holder at a 180° angle and both at a 90° angle with respect to the red laser irradiation direction. The filter holder between cuvette holder and detector was in a position without a filter (Figure S2, item 8). Luminescence emission spectra were measured using the same detector but with the UV−vis light source switched off. To visualize the spectrum from 450 to 950 nm, while blocking the red excitation light, a Thorlabs NF-633 notch filter was used in the variable filter holder. All spectra were recorded with Avasoft software from Avantes and further processed with Microsoft Office Excel 2010 and Origin Pro 9.1 software. Temperature dependent luminescence experiments were done with continuous irradiation and temperature ramping, except for phosphorescence measurements of compound **1** to prevent bleaching during the experiment. Instead, spectra were taken every 5 °C with 10 min thermal equilibration between temperature points.

Determination of the Quantum Yield of Upconversion. The absolute quantum yield of upconversion was determined by means of an integrating sphere setup. The setup and measurement procedure are discussed in depth in the Supporting Information.

RESULTS AND DISCUSSION

Neutral PEGylated liposome dispersions were prepared in phosphate buffered saline (PBS) by hydration and extrusion of lipid films containing six different neutral phosphatidylcholines, i.e., 1,2-dioleyl-*sn*-glycero-3-phosphocholine (DOPC), 1,2-dilaureyl-*sn*-glycero-3-phosphocholine (DLPC), 1,2-dimyristoyl-*sn*-glycero-3-phosphocholine (DMPC), 1,2-dipentadecanoyl-*sn*-glycero-3-phosphocholine (DPDPC), 1,2-dipalmitoyl-*sn*-glycero-3-phosphocholine (DPPC), and 1,2-distearoyl-*sn*-glycero-3-phosphocholine (DSPC) and in the presence of 4 mol % of sodium *N*-(carbonyl-methoxypolyethylene glycol-2000)-1,2-dis-

DOI: 10.1021/acs.jpcb.6b10039
J. Phys. Chem. B 2017, 121, 780−786

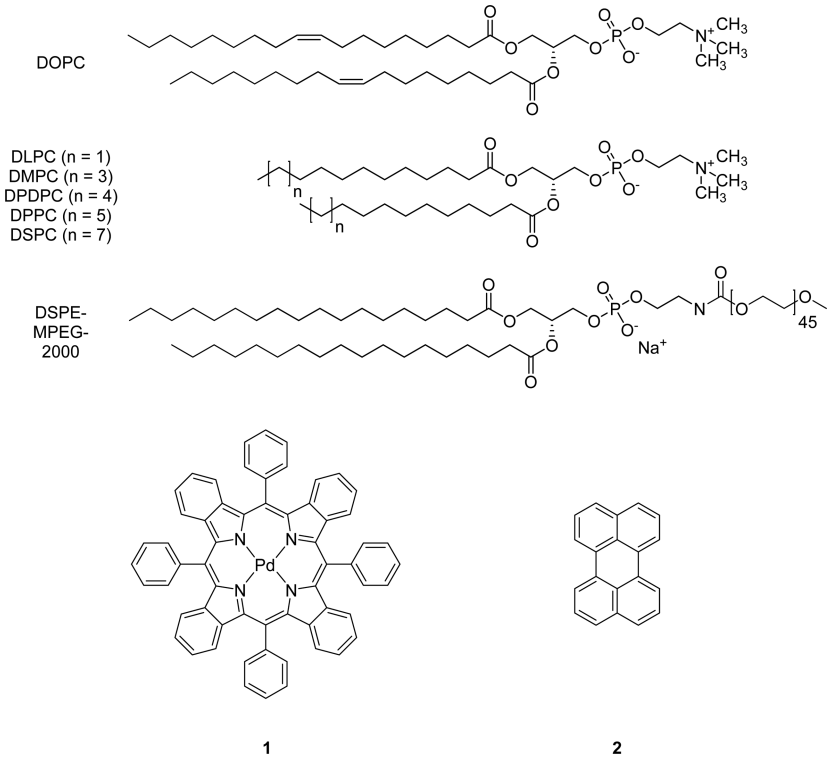

Figure 1. Chemical structures of DOPC, DLPC, DMPC, DPDPC, DPPC, DSPC, DSPE-mPEG-2000, palladium tetraphenyltetrabenzoporphyrin (**1**), and perylene (**2**).

Table 1. Lipid Formulations of the PEGylated Phosphatidylcholine Liposomes Used in This Work, and Their Physical Characterization by Dynamic Light Scattering (with *z*-ave as Hydrodynamic Diameter and PDI as Polydispersity Index) and Differential Scanning Calorimetry[a]

sample	lipid[b]	[**1**] (μM)	[**2**] (μM)[c]	*z*-ave (nm)	PDI	T_m (lit. value)[d,15] (°C)	ΔH (lit. value)[d,15] (kJ mol^{-1})
O	DOPC	-	-	139	0.11	- (−18.2)	- (35.5)
O1	DOPC	2.5	-	-	-	-	-
O2	DOPC	-	25	-	-	-	-
O12	DOPC	2.5	25	135	0.11	-	-
L	DLPC	-	-	127	0.11	- (−2.1)	- (7.5)
L12	DLPC	2.5	25	134	0.12	-	-
M	DMPC	-	-	132	0.07	25.0 (23.9)	27.7 (29.3)
M1	DMPC	2.5	-	-	-	-	-
M2	DMPC	-	25	-	-	-	-
M12	DMPC	2.5	25	134	0.09	24.9	26.6
PD	DPDPC	-	-	132	0.09	34.9 (34.7)	33.6 (32.7)
PD12	DPDPC	2.5	25	140	0.07	34.6	32.0
P	DPPC	-	-	140	0.08	42.4 (41.4)	40.1 (36.8)
P12	DPPC	2.5	25	137	0.11	42.1	38.7
S	DSPC	-	-	150	0.08	54.7 (55.2)	46.1 (48.3)
S12	DSPC	2.5	25	147	0.05	54.7	45.6

[a]DSC measurements were performed with a scanning rate of 1 °C min^{-1} at 3 atm pressure. [b]All liposomes were prepared with 5.0 mM lipid and 0.20 mM DSPE-mPEG-2000 in PBS (without sulfite). [c]Compound **2** was incorporated at 0.5 mol % with respect to the phospholipid; higher dye contents could not be reproducibly obtained with our liposome preparation method. [d]T_m is defined as the main transition temperature of the bilayer, and ΔH as the molar enthalpy change of the phase transition (the enthalpy change of the pretransition is included, in case there is one). Literature T_m and ΔH values given for the pure phospholipids.

tearoyl-*sn*-glycero-3-phosphoethanolamine (DSPE-mPEG-2000, see Figure 1). Addition of DSPE-mPEG-2000 is a well-known strategy to prevent liposome aggregation and fusion,[13] and moreover increases the hydrophobic dye loading capacity of phospholipid membranes.[14] The lipid composition of liposome samples **O**, **L**, **M**, **PD**, **P**, and **S** is shown in Table 1. A well-investigated red-to-blue TTA-UC dye couple consisting of palladium tetraphenyltetrabenzoporphyrin (**1**) and perylene (**2**, see Figure 1) was selected for incorporation in the lipid bilayer of the liposomes. Samples containing these dyes, i.e., **O12**, **L12**, **M12**, **PD12**, **P12**, and **S12** (defined in Table 1), were prepared following an identical procedure. The hydrodynamic diameters (*z*-ave = 137 ± 6 nm) and polydispersity indices (PDI = 0.09 ± 0.02), as measured by dynamic light scattering (DLS), were

DOI: 10.1021/acs.jpcb.6b10039
J. Phys. Chem. B 2017, 121, 780−786

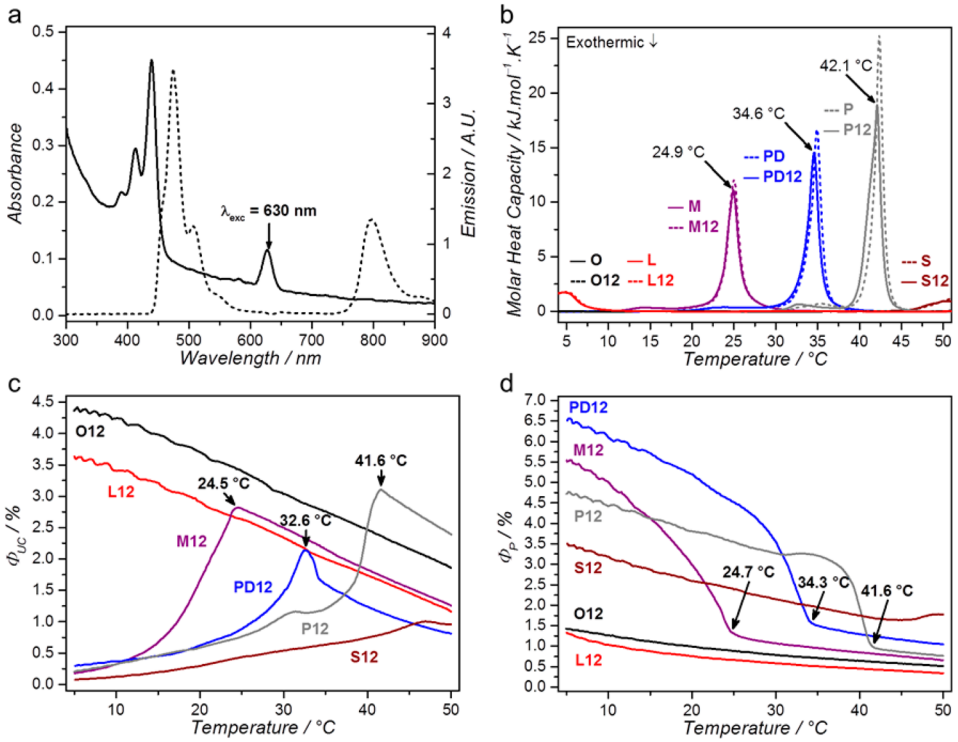

Figure 2. (Photo)physical characterization of upconverting liposomes. (a) Typical absorption (solid, left axis) and emission spectrum (dashed, right axis, λ_{exc} = 630 nm, intensity 80 mW cm^{-2}) of **L12** liposomes ([DLPC] = 1.0 mM, [**1**] = 0.5 μM, [**2**] = 5 μM) at 20 °C in 0.3 M sodium sulfite PBS under air. (b) Differential scanning calorimetry thermograms between 5 and 50 °C of liposomes with TTA-UC dyes (**O12**, **L12**, **M12**, **PD12**, **P12**, and **S12**, solid) or without (**O**, **L**, **M**, **PD**, **P**, and **S**, dashed). The thermograms for liposomes **S** and **S12** were recorded between 35 and 65 °C (Figure S3). Arrows indicate T_m of the dyed liposomes, where applicable. Measurements were performed in heating mode with a scanning rate of 1 °C min^{-1} at 3 atm pressure. (c,d) Temperature evolution of the upconversion quantum yield (Φ_{UC}, c) and of the residual sensitizer phosphorescence quantum yield (Φ_P, d) of **O12**, **L12**, **M12**, **PD12**, **P12**, and **S12**. Samples were heated from 5 to 50 °C at a rate of 1 °C min^{-1} while continuously irradiated with 80 mW cm^{-2} 630 nm light, at 1.0 mM lipid and [**1**] = 0.5 μM and [**2**] = 5 μM.

found to be very similar regardless of the lipid type or dye concentration.

It is well-known that phase changes of phospholipid membranes greatly influence the two-dimensional translational molecular diffusion coefficient (D_T in μm^2 s^{-1}) of membrane solutes. Therefore, the gel-to-liquid phase transition temperature (T_m) and the total enthalpy change of the phase transition (ΔH) were measured for samples based on DMPC, DPDPC, DPPC, and DSPC using differential scanning calorimetry (DSC, see Table 1, Figure 2b, and Figure S3). T_m and ΔH for dye-free PEGylated liposomes **M**, **PD**, **P**, and **S** were found to be very close to literature values for PEG-free liposomes, i.e., the PEG groups did not significantly influence the phase transition at these concentrations. Upon functionalization of the PEGylated liposomes with compounds **1** and **2**, a small decrease in the main transition peak height was observed, but the main features of the thermogram remained. These results indicate that for liposome samples **M12**, **PD12**, **P12**, and **S12** compounds **1** and **2** were indeed buried in the lipid bilayer, and that their presence only minimally perturbed the physical properties of the membranes. No transitions were found between 5 and 50 °C for samples **O**, **O12**, **L**, and **L12**, because T_m for pure DOPC and DLPC are reported to be below the freezing point of water.[15]

Next, UV−vis absorption and emission spectroscopy was performed on samples **O12**, **L12**, **M12**, **PD12**, **P12**, and **S12** at 20 °C in the presence of 0.3 M sodium sulfite (Figure 2).[5a,16] In these samples, sodium sulfite is used to chemically remove dioxygen. Earlier work showed that despite the large increase in buffer ionic strength, Na_2SO_3 does not affect the formation of DOPC and DMPC upconverting liposomes and allows stable TTA-UC to occur in air.[16b] Moreover, preliminary studies indicated that a 1:10 dye ratio (**1**:**2** = 0.05:0.50 mol % with respect to the lipid) resulted in optimized upconversion in **M12**, while higher dye-loading was severely limited by the solubility of **2** in the membrane. The absorption spectra of these samples showed the superposition of the characteristic bands of **1** at 440 and 630 nm and the vibronically structured band of **2** from 350−450 nm.[5b] Upon irradiation with 630 nm laser light (10 mW, 80 mW cm^{-2}), phosphorescence of **1** at 800 nm and upconversion emission of **2** at 474 nm were observed for each sample. The emission stability at 20 °C was tested for each formulation by continuously irradiating for 1 h and collecting emission spectra. All samples exhibited good emission stability during this period (Figure S4). The absolute quantum yield of upconversion (Φ_{UC}, 420−610 nm) and residual sensitizer phosphorescence (Φ_P, 725−950 nm), defined by the number of emitted photons divided by the number of absorbed photons (Supporting Information), was determined by means of an integrating sphere setup at room temperature (21.3 °C). Φ_{UC} had values of 3.6%, 2.8%, 2.0%, 0.7%, 0.6%, and 0.3% for **O12**, **L12**, **M12**, **PD12**, **P12**, and **S12**, respectively. This trend is in accordance with the findings of Poznik et al., who show that the upconversion intensity of green-to-blue TTA-UC in liposomes decreases strongly when going from DOPC to DMPC, while no upconversion was observed at all in DSPC.[17] Thus, the fact that we observe TTA-UC in the long-chained saturated phospholipids (i.e., DPDPC, DPPC, DSPC) at room temperature is interesting in itself. This may be explained by the longer

DOI: 10.1021/acs.jpcb.6b10039
J. Phys. Chem. B 2017, 121, 780−786

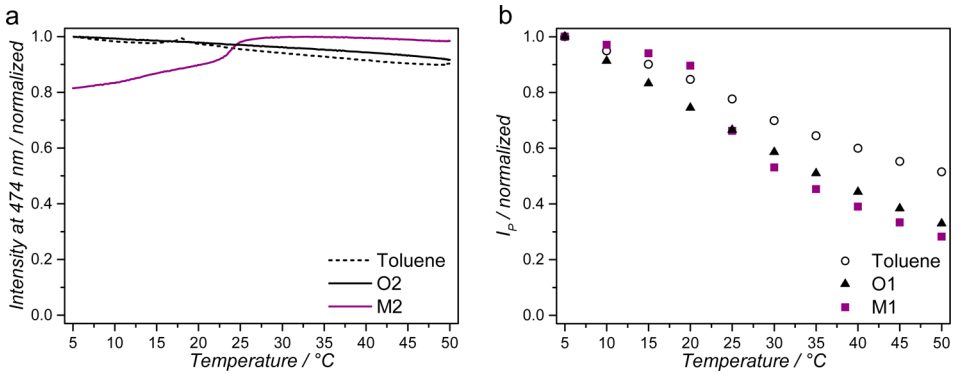

Figure 3. Temperature-dependent emission spectroscopy of compounds **2** or **1** in toluene, DMPC liposomes, or DOPC liposomes. (a) Normalized fluorescence intensity at 474 nm of compound 2 in toluene (dashed, 20 μM), **M2** liposomes (purple, [DMPC] = 1 mM), or **O2** liposomes (black, [DOPC] = 1 mM) as a function of temperature. λ_{exc} = 420 nm, 0.7 mW (6 mW cm^{-2}). (b) Temperature variation of the normalized phosphorescence intensity at 800 nm in 5 °C intervals for compound **1** in toluene under argon (open circles) and for liposomes **O1** (black triangles, [DOPC] = 1 mM) or **M1** (purple squares, [DMPC] = 1 mM) prepared in PBS with 0.3 M sodium sulfite. λ_{exc} = 630 nm, 10 mW (80 mW cm^{-2}).

triplet lifetimes (τ_T) of sensitizer **1** (τ_T = 250 μs in DMF)[18] compared to the green-absorbing sensitizer platinum octaethylporphyrin (PtOEP, τ_T = 50 μs in toluene),[19] which increases the possibility for TTA-UC.

To investigate the temperature dependency of TTA-UC in **O12**, **L12**, **M12**, **PD12**, **P12**, and **S12**, these samples were heated from 5 to 50 °C at a rate of 1 °C.min^{-1} while stirring, and upconversion spectra were continuously recorded. The same samples were used as for the quantum yield determination—these measurements were conducted within 24 h of each other. A submerged thermocouple registered the accurate temperature inside the solution. Figure 2 shows the evolution of Φ_{UC} and Φ_P vs temperature for each liposome formulation. These curves were obtained by recording the intensity of phosphorescence (I_P) and upconversion (I_{UC}) vs temperature and scaling these to the measured absolute quantum yields at 21.3 °C (vide supra). For **O12** and **L12**, both Φ_{UC} and Φ_P gradually decreased with increasing temperature. For **M12**, **PD12**, and **P12**, Φ_{UC} increased up to 25, 33, and 42 °C, respectively, and then decreased gradually, whereas Φ_P decreased steeply up to 25, 34, and 42 °C, respectively, and then continued to decrease, but less steeply. For **S12**, Φ_{UC} increased and Φ_P decreased with increasing temperature. When the samples were brought back from 50 to 5 °C, the initial emission spectra at 5 °C were obtained again in all cases (Figure S5) and the UV−vis absorption spectra were identical to those obtained at the beginning of these experiments (Figure S6); both findings showing that bleaching did not occur and that the thermophotophysical evolution is reversible. The shape of the observed temperature behavior was nearly identical at 5× lower concentration for **M12**, showing that the influence of liposome scatter is negligible (Figure S7). Also, in a control experiment in which DSPE-mPEG-2000 was omitted from sample **M12**, the shape of the observed temperature behavior was very similar, which indicates that PEGylation did not have significant influence on the observed thermophotophysical behavior (Figure S8). Interestingly, for **M12**, **PD12**, and **P12**, the temperature values at which Φ_{UC} maximizes and Φ_P kinks are very close to the phase transition temperature of the bilayer (T_m) recorded with DSC.

The increase of Φ_{UC} when approaching T_m is easily explained: heating the liposomes below T_m greatly increases the membrane fluidity and thus increases the lateral diffusion coefficient (D_T) of membrane dyes, which in turn causes an increase in TTA-UC efficiency. For instance, the D_T for fluorescent probes in DMPC lipid bilayers has been reported to increase from 0.01 μm^2 s^{-1} at 15 °C to 6 μm^2 s^{-1} at 30 °C to 13 μm^2 s^{-1} at 50 °C.[15,20] It is worth mentioning that for such DMPC bilayers, the foremost change in D_T (a three-order increase in magnitude) was found between 20 and 25 °C,[20] and so the most considerable transition in TTA-UC efficiency was expected to occur in this temperature domain. This is indeed in accordance with our data for **M12**. In the absence of accurate literature data of D_T in DPDPC and DPPC across the full temperature range, we assume that the same explanation holds for the results obtained with **PD12** and **P12**. However, this rationale is clearly no longer valid above T_m: although D_T continues to increase (vide supra), Φ_{UC} decreased. Furthermore, for **O12** and **L12**, in absence of a phase transition between 5 and 50 °C, Φ_{UC} and Φ_P both decrease across the entire temperature range. It is thus clear that other photophysical phenomena must play a role in the temperature dependence of TTA-UC in lipid bilayers.

Therefore, the thermophotophysical behavior of the isolated dyes was considered in DOPC, DMPC, and toluene (Figure 3). First, the fluorescence intensity of compound **2** (λ_{exc} = 420 nm, λ_{em} = 474 nm) was found to decrease by 10% in both DOPC liposomes and toluene when heated from 5 to 50 °C. This is most likely explained by a slightly increased thermal deactivation. In DMPC, the fluorescence intensity increased by 25% when heated from 5 to 30 °C, with the most sharp increase around 25 °C, and then decreased slightly again up to 50 °C. In all three systems, no significant spectral fluorescence differences are observed between 5 and 50 °C (Figure S9). This observation is in agreement with the work of Khan et al., who reported that perylene tends to form staggered nonfluorescent aggregates in the tightly packed gel membrane below T_m, which break apart in the more loosely packed liquid-crystalline state above T_m.[21] Since the fluorescence intensity is lower in the presence of such aggregates, the TTA-UC efficiency is lower below T_m. Overall, dissociation of perylene aggregates gives an additional explanation for the increase of upconversion intensity up to T_m.

Second, the phosphorescence intensity of **1** (λ_{exc} = 630 nm, λ_{em} = 800 nm) was investigated under deoxygenated conditions. In toluene solution, roughly 50% of the phosphorescence intensity is lost upon going from 5 to 50 °C due to increased thermal deactivation. When the dye was inserted into DOPC or DMPC liposomes (**O1** and **M1**, respectively) about 70% phosphorescence intensity was lost upon going from 5 to 50 °C; the additional 20% loss of phosphorescence intensity with respect to

DOI: 10.1021/acs.jpcb.6b10039
J. Phys. Chem. B 2017, 121, 780−786

the toluene sample may be due to increased dynamic self-quenching, because the molecules are much more confined in the lipid bilayer. The explanation of self-quenching is supported by the fact that, for **M1**, the highest loss of phosphorescence is observed around the transition temperature, at which the fluidity of the membrane increases most rapidly and diffusion-based processes such as self-quenching are expected to have an increased effect. Overall, these results explain that the decrease of TTA-UC with rising temperature is most likely due to increased thermal deactivation and self-quenching of **1**.

Based on these data, we explain the typical maximization of Φ_{UC} around T_m in lipid bilayers that have a transition temperature between 5 and 50 °C as follows. On one hand, the increase in photosensitizer quenching as a function of temperature is rather linear (Figure 3). On the other hand, the temperature dependence of D_T has been described in the literature as sigmoidal, with three orders of magnitude increase when approaching T_m, and flattening directly after T_m.[20] In other words, upon approaching T_m the membrane becomes fluid rather quickly, but once it reaches the liquid crystalline state the fluidity changes negligibly. Therefore, above T_m the effect of the only minor increase in lateral diffusion coefficient on the upconversion efficiency is completely outcompeted by the increased quenching of the photosensitizer. Furthermore, the dissociation of annihilator aggregates results in a rather abrupt and significant increase in fluorescence around T_m as well (Figure 3a). It is thus concluded that the combination of these three temperature-dependent phenomena results in the maxima that were observed in the Φ_{UC} versus temperature curve at 25, 33, and 42 °C for samples **M12**, **PD12**, and **P12**, respectively (Figure 2c).

Finally, for the biological application of these upconverting liposomes in bioimaging or phototherapy, it would be beneficial to achieve the highest upconversion intensity at human body temperature (37 °C). From our results, it is evident that the systems **O12**, **L12**, and **M12** achieve similar upconversion quantum yields at 37 °C, while **PD12**, **P12**, and **S12** exhibit lower quantum yields. Altogether, the results suggest that even though Φ_{UC} maximizes around T_m (for **M12**, **PD12**, and **P12**), choosing a lipid with a T_m near 37 °C does not result in an optimized upconverting liposome formulation. Finally, considering that little has been reported about the biocompatibility of DLPC, we conclude that **O12** and **M12** upconverting liposomes are the most promising for biological applications.

CONCLUSION

The temperature dependence of red-to-blue TTA-UC was studied in PEGylated liposomes with PC lipids with different lipophilic chain lengths and transition temperatures, and it was found that the upconversion efficiency maximizes around the order−disorder transition temperature of the membrane, T_m. Three major effects contribute to this temperature dependency: (1) an increase in lipid bilayer fluidity above T_m results in higher diffusion rates and thus in higher rates of TTET and TTA and higher upconverted intensity; (2) perylene aggregates dissociate when T approaches T_m, which results in higher annihilator emission intensity; and (3) higher thermal deactivation and self-quenching rates of the photosensitizer at higher temperatures lead to a lower TTET rate and lower upconversion intensity beyond T_m. Measuring the point at which I_{UC} maximizes may be exploited for probing the transition temperature of phospholipid membranes. Furthermore, for TTA-UC applications that require high performance at elevated temperatures, the results underline the importance of selecting photosensitizers that are minimally affected by temperature. Finally, the upconverted intensity in DOPC, DLPC, and DMPC liposomes were very similar at 37 °C, which highlights that not being at the optimum temperature for a given lipid composition does not necessarily mean that the upconverted intensity is lower than when being at the optimum temperature for another lipid composition. Overall, TTA-UC in liposomes can be realized with many different lipids of different T_m, and for both saturated and unsaturated lipids. For applications in bioimaging and phototherapy, the phospholipid can be rather freely chosen among DLPC, DMPC, and DOPC, while DPPC, DPDPC, and DSPC lead to slightly lower upconverted intensities. Such versatility allows for further optimizing the liposomal formulation in terms of other properties such as stability to medium, biocompatibility, toxicity, clearance from the bloodstream, and/or surface functionalization.

ASSOCIATED CONTENT

Supporting Information

The Supporting Information is available free of charge on the ACS Publications website at DOI: 10.1021/acs.jpcb.6b10039.

Mechanism of TTA−UC, emission spectroscopy setup, differential scanning calorimetry, temporal stability of upconversion and sensitizer phosphorescence, emission and absorption spectra, influence of sample concentration and PEGylation on recorded temperature dependence, determination of quantum yield of upconversion (PDF)

AUTHOR INFORMATION

Corresponding Author

*E-mail: bonnet@chem.leidenuniv.nl.

ORCID

Sylvestre Bonnet: 0000-0002-5810-3657

Notes

The authors declare no competing financial interest.

ACKNOWLEDGMENTS

This work was supported by the Dutch Organization for Scientific Research (NWO-CW) via a VIDI grant to S.B. The European Research Council is kindly acknowledged for a Starting Grant to S.B. Prof. E. Bouwman is gratefully acknowledged for her support and input. The COST action CM1105 "Functional metal complexes that bind to biomolecules" is gratefully acknowledged for stimulating scientific discussion. G. B. acknowledges the FNRS (FRFC 2010: 2.4592.10F) and the Van Buuren Foundation for the funding of the microcalorimetry equipment. COST action CM1005 (Supramolecular Chemistry in Water) is acknowledged for an STSM travel grant to S.H.C.A.

REFERENCES

(1) (a) Liu, Q.; Feng, W.; Yang, T.; Yi, T.; Li, F. Upconversion luminescence imaging of cells and small animals. *Nat. Protoc.* **2013**, *8* (10), 2033−2044. (b) Kim, J.-H.; Kim, J.-H. Encapsulated Triplet−Triplet Annihilation-Based Upconversion in the Aqueous Phase for Sub-Band-Gap Semiconductor Photocatalysis. *J. Am. Chem. Soc.* **2012**, *134* (42), 17478−17481. (c) Mahato, P.; Monguzzi, A.; Yanai, N.; Yamada, T.; Kimizuka, N. Fast and long-range triplet exciton diffusion in metal-organic frameworks for photon upconversion at ultralow excitation power. *Nat. Mater.* **2015**, *14* (9), 924−930.

(2) (a) Islangulov, R. R.; Kozlov, D. V.; Castellano, F. N. Low power upconversion using MLCT sensitizers. *Chem. Commun.* **2005**, *30*, 3776−3778. (b) Baluschev, S.; Miteva, T.; Yakutkin, V.; Nelles, G.;

DOI: 10.1021/acs.jpcb.6b10039
J. Phys. Chem. B 2017, 121, 780−786

Yasuda, A.; Wegner, G. Up-Conversion Fluorescence: Noncoherent Excitation by Sunlight. *Phys. Rev. Lett.* **2006**, *97* (14), 143903.
(3) (a) Majek, M.; Faltermeier, U.; Dick, B.; Pérez-Ruiz, R.; Jacobi von Wangelin, A. Application of Visible-to-UV Photon Upconversion to Photoredox Catalysis: The Activation of Aryl Bromides. *Chem. - Eur. J.* **2015**, *21* (44), 15496−15501. (b) Kwon, O. S.; Kim, J. H.; Cho, J. K.; Kim, J. H. Triplet-triplet annihilation upconversion in CdS-decorated SiO2 nanocapsules for sub-bandgap photocatalysis. *ACS Appl. Mater. Interfaces* **2015**, *7* (1), 318−25.
(4) (a) Monguzzi, A.; Borisov, S. M.; Pedrini, J.; Klimant, I.; Salvalaggio, M.; Biagini, P.; Melchiorre, F.; Lelii, C.; Meinardi, F. Efficient Broadband Triplet-Triplet Annihilation-Assisted Photon Upconversion at Subsolar Irradiance in Fully Organic Systems. *Adv. Funct. Mater.* **2015**, *25* (35), 5617−5624. (b) Nattestad, A.; Simpson, C.; Clarke, T.; MacQueen, R. W.; Cheng, Y. Y.; Trevitt, A.; Mozer, A. J.; Wagner, P.; Schmidt, T. W. An Intermediate Band Dye-sensitised Solar Cell Using Triplet-Triplet Annihilation. *Phys. Chem. Chem. Phys.* **2015**, *17*, 24826. (c) Hill, S. P.; Banerjee, T.; Dilbeck, T.; Hanson, K. Photon Upconversion and Photocurrent Generation via Self-Assembly at Organic−Inorganic Interfaces. *J. Phys. Chem. Lett.* **2015**, *6* (22), 4510−4517. (d) Nattestad, A.; Cheng, Y. Y.; MacQueen, R. W.; Schulze, T. F.; Thompson, F. W.; Mozer, A. J.; Fückel, B.; Khoury, T.; Crossley, M. J.; Lips, K.; Wallace, G. G.; Schmidt, T. W. Dye-Sensitized Solar Cell with Integrated Triplet−Triplet Annihilation Upconversion System. *J. Phys. Chem. Lett.* **2013**, *4* (12), 2073−2078.
(5) (a) Askes, S. H. C.; Kloz, M.; Bruylants, G.; Kennis, J. T.; Bonnet, S. Triplet-triplet annihilation upconversion followed by FRET for the red light activation of a photodissociative ruthenium complex in liposomes. *Phys. Chem. Chem. Phys.* **2015**, *17* (41), 27380−90. (b) Askes, S. H. C.; Bahreman, A.; Bonnet, S. Activation of a Photodissociative Ruthenium Complex by Triplet−Triplet Annihilation Upconversion in Liposomes. *Angew. Chem., Int. Ed.* **2014**, *53* (4), 1029−1033.
(6) (a) Nagai, A.; Miller, J. B.; Kos, P.; Elkassih, S.; Xiong, H.; Siegwart, D. J. Tumor Imaging Based on Photon Upconversion of Pt(II) Porphyrin Rhodamine Co-modified NIR Excitable Cellulose Enhanced by Aggregation. *ACS Biomater. Sci. Eng.* **2015**, *1* (12), 1206−1210. (b) Wohnhaas, C.; Mailänder, V.; Dröge, M.; Filatov, M. A.; Busko, D.; Avlasevich, Y.; Baluschev, S.; Miteva, T.; Landfester, K.; Turshatov, A. Triplet−Triplet Annihilation Upconversion Based Nanocapsules for Bioimaging Under Excitation by Red and Deep-Red Light. *Macromol. Biosci.* **2013**, *13* (10), 1422−1430. (c) Liu, Q.; Yin, B.; Yang, T.; Yang, Y.; Shen, Z.; Yao, P.; Li, F. A General Strategy for Biocompatible, High-Effective Upconversion Nanocapsules Based on Triplet−Triplet Annihilation. *J. Am. Chem. Soc.* **2013**, *135* (13), 5029−5037. (d) Kwon, O. S.; Song, H. S.; Conde, J.; Kim, H.-i.; Artzi, N.; Kim, J.-H. Dual-Color Emissive Upconversion Nanocapsules for Differential Cancer Bioimaging In Vivo. *ACS Nano* **2016**, *10* (1), 1512−21.
(7) (a) Zhou, J.; Liu, Q.; Feng, W.; Sun, Y.; Li, F. Upconversion Luminescent Materials: Advances and Applications. *Chem. Rev.* **2015**, *115* (1), 395−465. (b) Singh-Rachford, T. N.; Castellano, F. N. Photon upconversion based on sensitized triplet−triplet annihilation. *Coord. Chem. Rev.* **2010**, *254* (21−22), 2560−2573.
(8) (a) Hisamitsu, S.; Yanai, N.; Kimizuka, N. Photon-Upconverting Ionic Liquids: Effective Triplet Energy Migration in Contiguous Ionic Chromophore Arrays. *Angew. Chem., Int. Ed.* **2015**, *54* (39), 11550−4. (b) Lee, S. H.; Thévenaz, D. C.; Weder, C.; Simon, Y. C. Glassy poly(methacrylate) terpolymers with covalently attached emitters and sensitizers for low-power light upconversion. *J. Polym. Sci., Part A: Polym. Chem.* **2015**, *53* (14), 1629−1639. (c) Duan, P.; Yanai, N.; Nagatomi, H.; Kimizuka, N. Photon Upconversion in Supramolecular Gel Matrices: Spontaneous Accumulation of Light-Harvesting Donor-Acceptor Arrays in Nanofibers and Acquired Air Stability. *J. Am. Chem. Soc.* **2015**, *137* (5), 1887−94. (d) Duan, P.; Yanai, N.; Kimizuka, N. Photon Upconverting Liquids: Matrix-Free Molecular Upconversion Systems Functioning in Air. *J. Am. Chem. Soc.* **2013**, *135* (51), 19056−19059. (e) Svagan, A. J.; Busko, D.; Avlasevich, Y.; Glasser, G.; Baluschev, S.; Landfester, K. Photon energy upconverting nanopaper: a bioinspired oxygen protection strategy. *ACS Nano* **2014**, *8* (8), 8198−207.
(9) (a) Kim, J.-H.; Kim, J.-H. Triple-Emulsion Microcapsules for Highly Efficient Multispectral Upconversion in the Aqueous Phase. *ACS Photonics* **2015**, *2* (5), 633−638. (b) Huang, Z.; Li, X.; Mahboub, M.; Hanson, K.; Nichols, V.; Le, H.; Tang, M. L.; Bardeen, C. J. Hybrid molecule-nanocrystal photon upconversion across the visible and near-infrared. *Nano Lett.* **2015**, *15* (8), 5552−7.
(10) (a) Simon, Y. C.; Weder, C. Low-power photon upconversion through triplet-triplet annihilation in polymers. *J. Mater. Chem.* **2012**, *22* (39), 20817−20830. (b) Monguzzi, A.; Mauri, M.; Bianchi, A.; Dibbanti, M. K.; Simonutti, R.; Meinardi, F. Solid-State Sensitized Upconversion in Polyacrylate Elastomers. *J. Phys. Chem. C* **2016**, *120* (5), 2609−2614.
(11) Singh-Rachford, T. N.; Lott, J.; Weder, C.; Castellano, F. N. Influence of Temperature on Low-Power Upconversion in Rubbery Polymer Blends. *J. Am. Chem. Soc.* **2009**, *131* (33), 12007−12014.
(12) Massaro, G.; Hernando, J.; Ruiz-Molina, D.; Roscini, C.; Latterini, L. Thermally switchable molecular upconversion emission. *Chem. Mater.* **2016**, *28*, 738.
(13) Sawant, R. R.; Torchilin, V. P. Liposomes as 'smart' pharmaceutical nanocarriers. *Soft Matter* **2010**, *6* (17), 4026−4044.
(14) (a) Dzieciuch, M.; Rissanen, S.; Szydłowska, N.; Bunker, A.; Kumorek, M.; Jamróz, D.; Vattulainen, I.; Nowakowska, M.; Róg, T.; Kepczynski, M. PEGylated Liposomes as Carriers of Hydrophobic Porphyrins. *J. Phys. Chem. B* **2015**, *119* (22), 6646−6657. (b) Kępczyński, M.; Nawalany, K.; Kumorek, M.; Kobierska, A.; Jachimska, B.; Nowakowska, M. Which physical and structural factors of liposome carriers control their drug-loading efficiency? *Chem. Phys. Lipids* **2008**, *155* (1), 7−15.
(15) Marsh, D. *Handbook of Lipid Bilayers*, 2nd ed.; Taylor & Francis Group, LLC: Boca Raton, FL, USA, 2013; pp 380, 483−484, 548−549.
(16) (a) Penconi, M.; Gentili, P. L.; Massaro, G.; Elisei, F.; Ortica, F. A triplet-triplet annihilation based up-conversion process investigated in homogeneous solutions and oil-in-water microemulsions of surfactant. *Photochem. Photobiol. Sci.* **2014**, *13*, 48−61. (b) Askes, S. H. C.; Lopez Mora, N.; Harkes, R.; Koning, R. I.; Koster, B.; Schmidt, T.; Kros, A.; Bonnet, S. Imaging the lipid bilayer of giant unilamellar vesicles using red-to-blue light upconversion. *Chem. Commun.* **2015**, *51* (44), 9137−9140.
(17) Poznik, M.; Faltermeier, U.; Dick, B.; Konig, B. Light upconverting soft particles: triplet-triplet annihilation in the phospholipid bilayer of self-assembled vesicles. *RSC Adv.* **2016**, *6* (48), 41947−41950.
(18) Vinogradov, S. A.; Wilson, D. F. Metallotetrabenzoporphyrins. New phosphorescent probes for oxygen measurements. *J. Chem. Soc., Perkin Trans. 2* **1995**, *0* (1), 103−111.
(19) Bansal, A. K.; Holzer, W.; Penzkofer, A.; Tsuboi, T. Absorption and emission spectroscopic characterization of platinum-octaethylporphyrin (PtOEP). *Chem. Phys.* **2006**, *330* (1−2), 118−129.
(20) Chang, C.-H.; Takeuchi, H.; Ito, T.; Machida, K.; Ohnishi, S.-i. Lateral Mobility of Erythrocyte Membrane Proteins Studied by the Fluorescence Photobleaching Recovery Technique. *J. Biochem.* **1981**, *90* (4), 997−1004.
(21) Khan, T. K.; Chong, P. L.-G. Studies of Archaebacterial Bipolar Tetraether Liposomes by Perylene Fluorescence. *Biophys. J.* **2000**, *78* (3), 1390−1399.

NOTE ADDED AFTER ASAP PUBLICATION

This paper published ASAP on 1/24/2017. The Acknowledgment section was modified and the revised version was reposted on 2/2/2017.

DOI: 10.1021/acs.jpcb.6b10039
J. Phys. Chem. B 2017, 121, 780−786